Determination of the $^{41}K/^{39}K$ $5^2P_{1/2}$ Isotope Shift and Analysis of Ground State Populations of Laser-Cooled ^{41}K

by

Landon Halloran
TRIUMF
4004 Wesbrook Mall
Vancouver, BC, Canada
V6T 2A3

Under Supervision by:
John A. Behr

Landon James Szasz Halloran

April 28, 2006

Physics and Astronomy Co-op Work Term Report
University of Victoria

1 Abstract

The isotope shift is the difference in energy between the same transition in two different isotopes. Presented here is the measurement, using saturation spectroscopy and lock-in amplification, of a $^{41}K/^{39}K$ $4S_{1/2} \rightarrow 5P_{1/2}$ isotope shift of 456.1±0.75MHz. By subtracting the known normal mass shift of 508.8MHz from this, a residual isotope shift of −52.7±0.75MHz is found. The specific mass shift of −39.4±5.13MHz, whose precision is limited by muonic X-ray data, is approximately double that of the $4S_{1/2} \rightarrow 4P_{1/2}$ transition. Additionally, the hyperfine A coefficient of the ^{41}K $5P_{1/2}$ state was measured to be 4.96±0.17MHz.

A separate analysis of the distribution of electrons to the different magnetic substates during optical pumping of ^{41}K in a MOT is also made. By linearly exciting electrons from the ground state to the $5P_{1/2}$ state with a pulsed, frequency-swept 405nm laser, photoionizing with a pulsed 532nm laser, and detecting the resulting photoions, the ground state populations are probed. It is clear from the results that the F=1 level is being preferentially populated in all three polarizations. A further analysis of the ground states is presented, noting the restrictions of the employed model.

Contents

List of Tables

List of Figures

2 Introduction

The TRIUMF Neutral Atom Trap (TRINAT) system has the ability to trap stable and radioactive isotopes in its magneto-optical (MOT) trap[18]. Previous and ongoing TRINAT experiments have studied ^{36}K, ^{37}K,^{38m}K, ^{39}K, ^{41}K, ^{78}Rb and ^{80}Rb. This work is limited to the stable Potassium-39 and Potassium-41 isotopes[1], but the analysis of polarization will have applications to other TRINAT experiments. Ongoing work is studying β decay, searching for parity symmetry violation, including right handed neutrinos, in trapped Potassium isotopes (see, for example, [4]). In order to complete analysis of the polarization of trapped atoms, not only the polarization, but also the distribution of ground-state populations during linear, σ^+ and σ^- polarized optical pumping with a 770nm diode laser needs to be understood. By trapping and polarizing ^{41}K, a study of the redistribution of electrons by polarized light, which optically pumps the $4s_{1/2} \rightarrow 4p_{1/2}$ transition, to the eight magnetic sublevels of the $4s_{1/2}$ state is made. The probing of these levels is done with a linearly-polarized 405nm laser, which excites the electrons to the $5P_{1/2}$ state.

A separate measurement of the ^{41}K/^{39}K isotope shift is also made. The isotope is the difference in a transition's energy between two isotopes of the same element. It is a result of the electron quantum state's overlap with the nucleus, which differs in mass and size between isotopes. This measurement was done using a 405nm laser for saturation spectroscopy. Of interest in the area of atomic physics is the field shift, which can be deduced from the isotope shift measured in this work and a scaled specific mass shift [14]. By making computational fits to the spectroscopic data, the hyperfine A coefficient can also be determined if the F$'$=1,2, as well as their crossover, peaks are fully resolved either directly, or in a well-understood lock-in signal. As the isotope shift, the resulting field shift component, and the hyperfine A coefficient for the $5P_{1/2}$ state have not been previously measured, a paper is in preparation summarizing these results [11].

[1]The natural abundance of ^{41}K is 6.73%; ^{39}K, 93.26%; and ^{40}K, 0.01%.

3 Theory

3.1 Level Splitting

3.1.1 Hyperfine Splitting

For an atom with quantum numbers $I = \frac{3}{2}$ and $J = \frac{1}{2}$, there exist eight substates within a given state, such as, in this work, the $4^2S_{1/2}$ and $5^2P_{1/2}$ states of ^{39}K and ^{41}K. The Hamiltonian operator, including the hyperfine interaction and a weak external magnetic field,

$$H = A\mathbf{I}\cdot\mathbf{J} + cJ_Z, \text{ where } c = \frac{\mu_B B_Z g_J}{h},$$

(where A is the hyperfine A coefficient; B_Z, the magnetic field along the quantization axis; g_J, the atomic g-factor; and h, the Planck constant) determines the mixing of sublevels. The dot product of the quantum vectors, **I** & **J** can be evaluated by

$$\mathbf{I}\cdot\mathbf{J} = I_Z J_Z + (1/2)(I_+ J_- + I_- J_+) \ .$$

The raising operator, L_+, and the lowering operator, L_-, where, in this case $L = I$ or J, effects the state on which it operates by raising or lowering the m_L quantum number by one and holding L constant:

$$L_\pm = \sqrt{L(L+1) - m_L(m_L+1)}|L, m_L \pm 1\rangle$$

For ^{39}K and ^{41}K, the result of solving the Hamiltonian is an 8x8 matrix with only six non-diagonal, non-zero terms. The Eigenvectors of this matrix give the degree of mixing of the sublevels. In the absence of a magnetic field, the mixing of states with the same F reduces to zero. In this situation, there are two energy levels, split by twice the hyperfine A coefficient: the states where $F = 1$, and those where $F = 2$. When a magnetic field is present, six of the eight sublevels will mix and there will be a difference in the energy of each sublevel in an effect called Zeeman-splitting (see Figure 1).

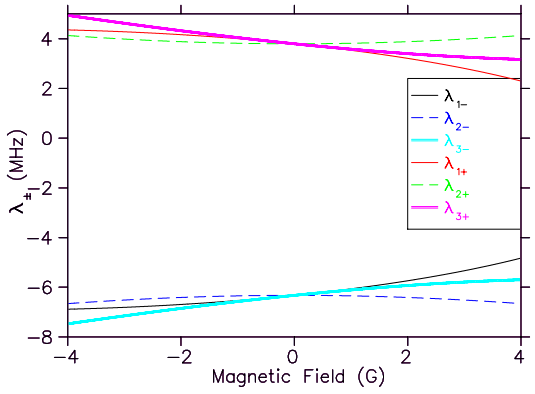

Figure 1: Level-mixing of $5p_{1/2}$ states in ^{41}K.

3.1.2 Zeeman-Split Sublevels

Zeeman splitting depends on an atom's magnetic moment, $\mu_B(g_l + g_s)$ (where g_l and g_s are the orbital and rotational g-factors, respectively), associated with the motion of the atom's electrons. The atom's nuclear magnetic moment is about three orders of magnitudes smaller due to the scaling of the nuclear magneton by the ratio of the electron mass to the nucleon mass (1/1836)[8]. As such, the effect of the nuclear magnetic moment is negligible for this experiment.

In the presence of a magnetic field, the electron energy level will increase or decrease due to the coupling of the magnetic moment with the field[8]. For low fields, this effect scales linearly with the magnetic field present along the quantization axis. In the TRINAT apparatus a quadrupole magnetic field is present in the MOT, along with a uniform bias field. The Zeeman splitting (see Figure 2) will become significant in ^{39}K and ^{41}K experiments as an aid in determining the ground-state populations of the electrons of the trapped atoms if the measured line-widths are small and the magnetic fields along the quantization axis sufficiently high.

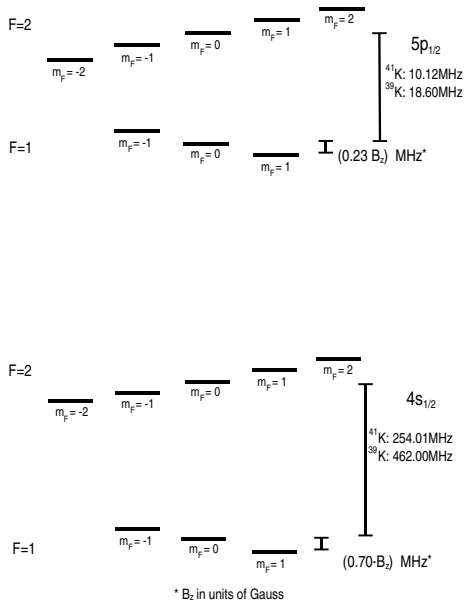

Figure 2: Zeeman and Hyperfine Split Energy levels of ^{39}K and ^{41}K

3.2 Probing Polarization and Ground-State Populations

Polarization of the atoms in the MOT redistributes the electrons of the trapped atoms to different energy levels. Polarization is a measure of the average value of the quantum number m_I. This is calculated using the Clebsh-Gordon coefficients (see Table 1). In perfect positive polarization, all of the electrons would be in the $F = 2$, $\mathrm{m}_F = 2$ state and the mean value of m_I would be $\frac{3}{2}$. In perfect negative polarization, all the electrons would occupy the $F = 2$, $\mathrm{m}_F = -2$ state and the mean value of m_I would be $-\frac{3}{2}$.

If the polarization is not perfect, knowledge of the polarization does not reveal the population distribution of the ground-state electrons. In order to determine this, data must be taken showing the absorption spectra of the atoms. In this work, atoms are trapped in a MOT and the number of ions resulting from photo ionization by laser light at known frequencies is recorded. As the intensity of the individual absorption peaks (see Figure 3) will depend on the ground-state populations of the electrons, computational fits of Lorentzian-distributed

Clebsh-Gordon coefficient	**F**	$\mathbf{m}_F$	$\mathbf{m}_I$	$\mathbf{m}_J$
1	2	-2	$-\frac{3}{2}$	$-\frac{1}{2}$
$\frac{\sqrt{3}}{2}$	2	-1	$-\frac{1}{2}$	$-\frac{1}{2}$
$\frac{1}{2}$	2	-1	$-\frac{3}{2}$	$\frac{1}{2}$
$\frac{1}{\sqrt{2}}$	2	0	$-\frac{1}{2}$	$\frac{1}{2}$
$\frac{1}{\sqrt{2}}$	2	0	$\frac{1}{2}$	$-\frac{1}{2}$
$\frac{1}{2}$	2	1	$\frac{3}{2}$	$-\frac{1}{2}$
$\frac{\sqrt{3}}{2}$	2	1	$\frac{1}{2}$	$\frac{1}{2}$
1	2	2	$\frac{3}{2}$	$\frac{1}{2}$
$\frac{1}{2}$	1	-1	$-\frac{1}{2}$	$-\frac{1}{2}$
$-\frac{\sqrt{3}}{2}$	1	-1	$-\frac{3}{2}$	$\frac{1}{2}$
$\frac{1}{\sqrt{2}}$	1	0	$\frac{1}{2}$	$-\frac{1}{2}$
$-\frac{1}{\sqrt{2}}$	1	0	$-\frac{1}{2}$	$\frac{1}{2}$
$\frac{\sqrt{3}}{2}$	1	1	$\frac{3}{2}$	$-\frac{1}{2}$
$-\frac{1}{2}$	1	1	$\frac{1}{2}$	$\frac{1}{2}$

Table 1: Clebsh-Gordon Coefficients for an Atom with Quantum Numbers $\mathbf{I} = \frac{3}{2}$ & $\mathbf{J} = \frac{1}{2}$

absorption peaks can be made to this data, resulting in a greater understanding of the electron distribution in the ground states.

Even with the same degree of polarization (same $\langle m_i \rangle$ value) for atoms in the MOT, there is a wide range of values of $\langle m_i^2 \rangle$ that are possible. $\langle m_i^2 \rangle$ (see Table 2 for the $\langle m_i^2 \rangle$ value of each substate) is sensitive to the distribution of electrons in the magnetic substates, $|F, m_F\rangle$. This sensitivity is very useful when making fits to data to determine if the polarizing beam is preferentially populating either the $F = 1$ or $F = 2$ sublevels.

3.3 Isotope Shifts

Isotope shift is the difference in energy between the same states of two different isotopes of the same element. The isotope shift is due primarily to the difference in overlap of the electron state with the nucleus, and the differing nuclear mass and size[13]. This can be broken into three components: the specific mass shift,

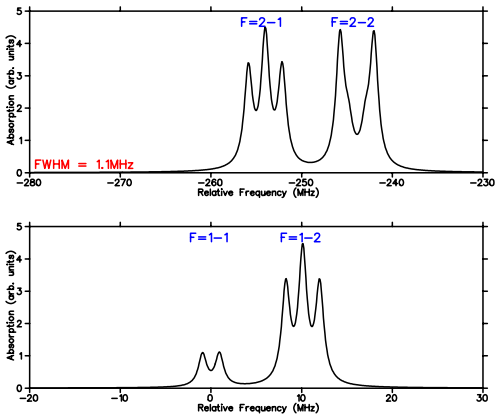

Figure 3: Expected Distribution of Absorption in ^{41}K for a 2Gauss Magnetic Field and a 1.1MHz Line Width

normal mass shift and the field shift.

The normal mass shift is a result of the difference in nuclear mass between two isotopes. It can be considered a zero-order approximation of the isotope shift. Where m is the electron mass, M_1 and M_2 are the nuclear masses of the lighter and heavier isotopes, and ν_1 is the frequency of the transition in the lighter isotope, the normal mass shift is

$NMS = (\frac{m(M_2-M_1)}{M_1(M_2+m)})\nu_1$ [9].

For the $4s_{1/2}$-$5p_{1/2}$ transition in ^{39}K and ^{41}K, whose atomic masses are $38.963707u$ and $40.961825u$, respectively, the normal mass shift is 508.8MHz. The specific mass shift is a much more involved calculation, drawing on many body perturbation theory. Currently, no comprehensive analysis is known to have been made of the $5p_{1/2}$ state. For the $4s_{1/2}$-$4p_{1/2}$ transition, the specific mass shift has been determined empirically to be -19.92±4.9MHz, and the field shift to be -12.91MHz [14]. It is known that the field shift component of the isotope shift is dominated by the ground state. By assuming that the specific mass

$\langle \mathbf{m_i^2} \rangle$	$\langle \mathbf{m_i} \rangle$	**F**	$\mathbf{m_F}$
$\frac{9}{4}$	$-\frac{3}{2}$	2	-2
$\frac{3}{4}$	$-\frac{3}{4}$	2	-1
$\frac{1}{4}$	0	2	0
$\frac{3}{4}$	$\frac{3}{4}$	2	1
$\frac{9}{4}$	$\frac{3}{2}$	2	2
$\frac{7}{4}$	$-\frac{5}{4}$	1	-1
$\frac{1}{4}$	0	1	-1
$\frac{7}{4}$	$\frac{5}{4}$	1	1

Table 2: $\langle m_i^2 \rangle$ & $\langle m_i \rangle$ of the Magnetic Substates of ^{39}K and ^{41}K

shift of the $5p_{1/2}$ state is less than or equal to that of the $4p_{1/2}$ state (as in Li calculations[13]), an initial estimate of 476.8MHz can be made for the ^{41}K/^{39}K isotope shift.

4 Experimental Techniques

4.1 Magneto-Optical Traps

Magneto-Optical Traps (MOT's) are systems in which atoms are confined to a region of space using beams of coherent light. The Nobel Prize for Physics was awarded to Steven Chu[6], Claude Cohen-Tannoudji[7], and William D. Phillips[17] in 1997 for its development. The first highly-successful MOT held 10^7 Sodium atoms at temperatures less than 1mK in a region less than 0.5mm across[18]. The major advantage of a MOT is that its mechanism of trapping, electromagnetic radiation, permits the trapping of neutral atoms.

The TRINAT apparatus used in this experiment consists of two MOTs linked together in a ultra-high vacuum (UHV) chamber. The first MOT is used to trap and cool atoms. These atoms are then moved by optical pumping to a second MOT. The second MOT has a much lower content of untrapped atoms and, as such, has a much lower rate of background counts[19]. In previous experiments involving radioactive isotopes [5], protons with energies of 500MeV were delivered via the ISAC[2] beamline to a target producing the isotope of interest.

[2]Isotope Separator & Accelerator

A 767nm Titanium-Sapphire (Ti:Sapph) laser is driven by a multi-line visible Argon-ion laser. The Ti:Sapph laser outputs ∼1.5W of coherent, single-wavelength light. It is locked (see Section 5.1) to a $4S_{1/2} \rightarrow 4P_{3/2}$ F_g=1 transition of ^{41}K. The frequency of the laser light is shifted via acousto-optical modulation and enters the MOT chamber red-detuned by 3-5Γ from a $4S_{1/2}$-$4P_{3/2}$ transition of ^{41}K. Counter-propagating beams with opposite circular polarizations pass through the MOT, coherently trapping atoms by creating a net force that decreases nearly linearly with velocity[18]. This permits the cooling of atoms with velocities lower than a threshold that depends on the laser light intensity, the detuning, and the spontaneous emission rate[3]. Counter-propagating beams with opposite polarizations travel in three orthogonal directions in the presence of a magnetic quadrupole field, meeting at the center of the MOT. The magnetic quadrupole field is kept on throughout the entire experiment to enable fast laser switching, preventing the atoms from moving. Due to its orientation, it causes states with the same F and different m_F to mix, complicating optical pumping. An additional uniform field applied with Helmholtz coils allows the sublevels to be Zeeman-split, providing a probe into the ground state populations of the trapped atoms.

The atoms are transfered via a 767nm push beam to the second MOT (see Figure 4 [3]). Here, they are polarized (see Section 4.3) with 767nm light. Linearly-polarized 405nm light (see Section 4.2) is used to excite the trapped atoms. Pulsed 532nm light photoionizes the excited atoms, which undergo an acceleration through a potential of 500-800V before hitting a microchannel plate (MCP) which sends a signal to the data collection system.

4.2 Acousto-Optic Modulation and 405nm beam paths

An acousto-optic modulator (AOM) modifies the frequency, path, and phase of a laser beam. An AOM uses the acousto-optic effect, in which high-frequency acoustic waves can couple the strain field to the index of refraction of a crystal[21]. The major advantage of acousto-optic modulation is that the frequency an output beam, ν', is shifted by an integer multiple of the input acoustic frequency,

[3] Figure adapted from [3].

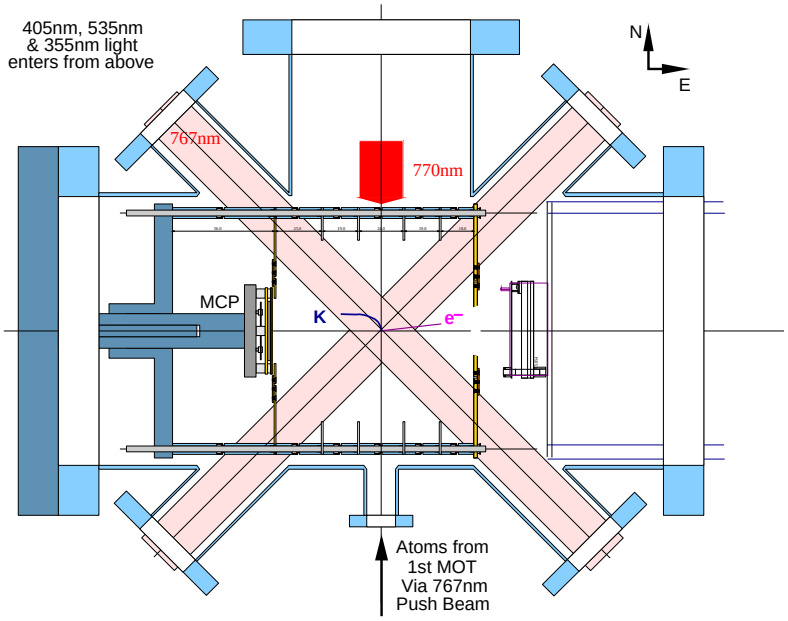

Figure 4: The MOT Used for Photoionization

f, from the input laser frequency, ν:

$$\nu' = \nu + nf,\ n = 0, 1, 2, 3 \ldots .$$

The output beams are also shifted in path direction by a given angle,

$$\theta = \arcsin\left(\frac{n\nu}{2f}\right) .$$

The intensity of each beam is highly sensitive to the input angle of the light and, as such, adjustments can be made to optimize the power in the output beam of interest. Generally, this is the first-order diffraction, the beam shifted by f. Beams other than this and the zero-order beam will have significantly less power.

In the TRINAT system, multiple AOM's are used to obtain more than one frequency of light from each of the 405nm, 767nm and 770nm lasers. The 405nm

laser set-up, with which this work is primarily concerned, contains an AOM capable of providing a shift of up to 380MHz that was used for two separate applications.

For the spectroscopic analysis of the ^{39}K and ^{41}K $4S_{1/2}$-$5P_{1/2}$ lines, the beam from the diode laser was split with a polarizing beam-splitter. One beam was sent through the spectroscopy cell and to a photodetector. The output of this photodetector was sent to a lock-in amplifier and was used to lock the laser to a strong ^{39}K line of known frequency. The beam that was reflected at 90° in the beam-splitter was double-passed through an AOM which provided a total frequency shift of $2f$. The frequency shift was controlled externally with an ADC connected to a PC. From the AOM, the beam was reflected through the spectroscopy cell and then back to a photodetector. The signal from this photodetector was sent to an external amplifier and lock-in amplifier (see Figure 5 [4]).

For the analysis of ground state populations, a polarizing beam-splitter was used to send ∼50% of the beam to the spectroscopy cell for laser locking and the rest to the double-pass AOM. The laser was locked to ^{39}K absorption lines from the cell, while the PC-controlled AOM shifted the beam that was sent to the MOT over the frequency range of interest.

In both cases, an adjustable aperture was used to block all beams other than the first-order beam. This beam was then reflected back through the AOM, providing it with another shift of f and sending it back along its original path.

4.3 Polarization of Atoms with Circularly-Polarized Light

The 770nm diode laser was used to polarize the ^{41}K atoms trapped in the MOT. It was frequency-locked to the $4P_{1/2}$ F=2-$\frac{1}{2}$ transition of ^{39}K with excellent long-term stability. The laser was frequency-shifted by direct frequency modulation[12] so that there was a $\sim \frac{1}{3}$ amplitude ratio of the sidebands to the main frequency (see Figure 6). The polarization of the laser light was controlled by a liquid crystal variable retarder, which effectively functions as a $\frac{\lambda}{4}$, $\frac{\lambda}{2}$, or

[4] adapted from [9]

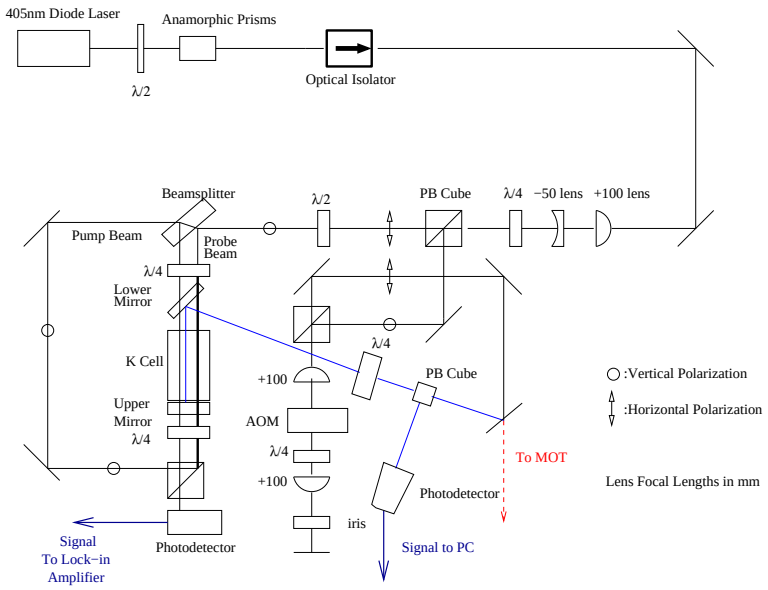

Figure 5: Beam Path For Spectroscopic Analysis of the Isotope Shift

$\frac{3\lambda}{4}$ wave plate, depending on the control signal. The carrier and side-bands are separated so that they excite the $4P_{1/2}$ F=2-2 and F=1-2 transitions of ^{41}K. This allows optical pumping of both $4P_{1/2}$ levels, leading to a higher degree of polarization. Linear polarization should not preferentially shift the population levels; it populates the magnetic sublevels of the same quantum number F nearly evenly. Circularly-polarized (σ) light redistributes the electrons to different magnetic sublevels (see Figure 7 [5]). σ^+ light shifts m_F by 1 for each transition from the ground to the excited state; likewise, σ^- shifts m_F by -1. When the electron decays back to the ground state, it retains its shifted m_F quantum number. After many iterations of this process, the atoms become po-

[5] adapted from [3]

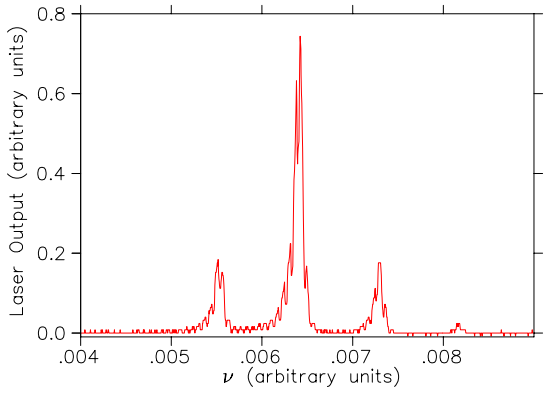

Figure 6: 770nm Laser Output with Sidebands from Direct Frequency Modulation

larized with redistributed ground-state population levels which are probed via the 405nm diode laser.

4.4 Photoionization and Detection

The 405nm diode laser is used to excite electrons from the $4S_{1/2}$ ground state to the $5P_{1/2}$ excited state (see Figure 8). The light is linearly polarized, so it will only excite $\Delta m_F = 0$ transitions. Pulsed 532nm laser light is sent to the MOT through the same orientation as the 405nm light and triggers the 405nm so that it is pulsed on for a time range that overlaps the 532nm pulse. Light from the 532nm laser ionizes the atoms in the excited state. Because the 532nm laser is pulsed, the ions produced by it can be distinguished by making time cuts in the data.

The 405nm laser is frequency-locked to a ^{39}K $4S_{1/2}$-$5P_{1/2}$ transition of known frequency (see Section 5.1) and is shifted via an AOM (see Section 4.2) so that the final frequency is known to high precision. When this shifted light is at the frequency of a resonance of the trapped ^{41}K atoms, it will excite the electrons linearly to the $5P_{1/2}$ state, retaining the original quantum numbers

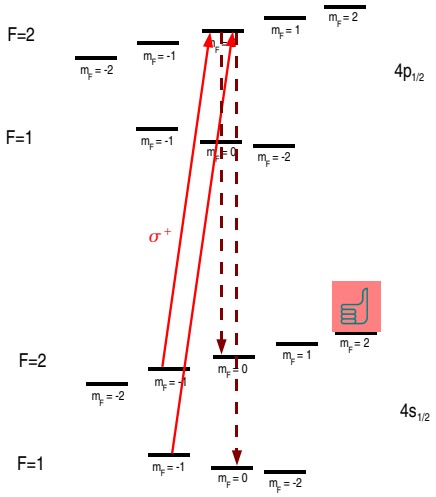

Figure 7: Polarization with 770nm σ^+ Light

F and m_F. After a photon from the pulsed 532nm laser ionizes the atom by further exciting the $5P_{1/2}$ electron to the continuum, the potassium ion is accelerated (see Figure 4) through an electric potential towards a microchannel plate. From the MCP data, the distribution of the atoms trapped in the MOT can be determined. By processing the data in conjunction with timing data from the lasers using the program NOVA[6], a myriad of information about the atoms in the MOT is obtained.

5 Discussion

5.1 Laser Locking

Lasers are designed to output single-wavelength, coherent light. Various factors, including acoustic noise and temperature fluctuations, cause the frequency of the light to drift somewhat randomly with time. TRINAT requires a constant

[6]See *http://www.usatlas.bnl.gov/computing/nova/*

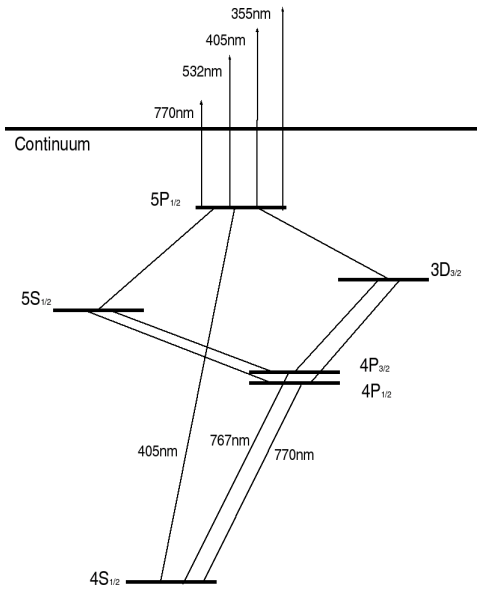

Figure 8: Possible Transitions in ^{39}K and ^{41}K Atoms with the TRINAT Set-Up.

frequency of light in order to excite the transition of interest. In order to achieve this stability, the technique of lock-in amplification[7] is used.

Three of the lasers in our experiment required frequency-locking: the Coherent[8] 767nm Titanium-Sapphire ring laser, the Toptica[9] 770nm diode laser, and the Toptica 405nm diode laser. All three lasers were locked using lock-in amplifiers.

Laser light is passed through a polarizing beam-splitter cube where ∼50% of the light is allowed to pass to the spectroscopy cell and the rest is reflected 90° and sent to the experiment. The light that passes through the polarizing beam-splitter passes through a half-wave plate which vertically polarizes the light (see Figure 5). A beamsplitter then splits the laser light into three different beams. Two of these beams are reflected at 90° and pass through a cell 10cm in length

[7] Also known as phase-sensitive detection.
[8] Coherent Inc., *http://www.coherentinc.com*
[9] Toptica Photonics AG, *http://www.toptica.com*

containing potassium which is kept at 70±4 °C; they act as probe beams and are at a low enough power that they will not saturate the transitions of interest. The majority of the light passes through the beamsplitting cube and is reflected in the opposite direction of one of the beam paths. This beam, the pump beam, is useful in Doppler-free spectroscopy[8] because it saturates the transition of interests. After the cell, the beam that shares its path with the pump beam hits a photodetector. In this case, since the hyperfine splittings of the transitions that the laser was locked to were <20MHz and the Doppler-broadening was >1500MHz FWHM, subtracting the Doppler-broadened Gaussian was not necessary. Had the hyper-fine splittings been greater, each probe beam would have been sent to a separate photodiode. One signal would have then been subtracted from the other through reverse-biasing, leaving a weaker signal absent of Doppler-broadened background. Some experimentation was made with this technique, but the single photodetector gave a stronger signal to which the laser could be locked with greater ease.

The laser is swept in frequency by varying the position of the grating in the laser cavity with a scan control module[10] that controls a piezoelectric transductor (PZT). The output of the photodetector is sent to an oscilloscope to display its signal as a function of scan control voltage (with which frequency varies nearly linearly in mode-hop free regions). From this, the peak to which a laser is to be locked can be found (see Appendix B.

The signal from the photodetector was also sent to the lock-in amplifier input. The lock-in amplifier modulates the Zeeman coil with a small sinusoidal variation, causing the frequency of the laser to shift sinusoidally. If the laser frequency is slightly below resonance, the absorption signal will be in phase with the modulation. If it is slightly above resonance, the absorption signal will be 180° out of phase with the modulation frequency. On resonance, the signal will be doubled in frequency as the laser sweeps both above and below the absorption peak once every period[20]. The lock-in module sends this signal through a "PID" loop which has controls for proportionality (sensitivity to the sign of the lock-in signal), integration, and differentiation. Many different

[10] For the two diode lasers, the Toptica SC110 was used as a scan control and the LIR100/110 as a lock-in module.

settings were used to obtain a stable lock of the 405nm laser. To optimize, the scan control amplitude was varied while different PID settings were used. The optimal PID settings kept the laser in lock even at high amplitudes of the scan control, which effectively acts as a fast drift of the laser frequency to which the lock-in must adjust. To maximize the lock-in signal, the phase of the modulation signal is varied until the signal is nearly zero, then the phase is adjusted 90°.

Raw signals from the photodetector with signal-to-noise (s/n) ratios less than two, and often less than one, were processed by a lock-in amplifier and resulted in lock-in signals with much higher s/n ratios to which the laser could be locked. Unfortunately, even with the optimized lock-in amplifier and PID settings, the laser could only be locked for periods of 2-30 minutes, primarily due to laser drift that caused the laser to hop from one lasing mode to another. To fix this, two components were constructed. A low-pass filter was connected to the scan control voltage to filter out 60Hz and higher-frequency noise that was unnecessarily raising the frequency width of the lock and causing increased instability. An acoustic shield to encase the laser housing was also constructed. Acoustic noise dropped by an average of ∼3dB over the 0-5kHz frequency range (see Figure 9). This also fortuitously improved the thermal stability of the laser, greatly reducing the long-term drift of laser frequency from tens of MHz per minute to a few MHz per minute. With these two components in place, the laser could be locked for several hours.

5.2 ^{41}K/^{39}K Isotope Shift from Laser Spectroscopy

The method described in section 4.2 was used to obtain absorption spectra of the ^{41}K F_g=2 peaks. The 405nm diode laser was frequency-locked to the cross-over resonance of the ^{39}K $4S_{1/2}$-$5P_{1/2}$, F_g=2 transitions. The F_g=2 transitions have the highest intensities of the $4S_{1/2}$-$5P_{1/2}$ transitions. These peaks were also the best resolved, and the zero-crossing of the cross-over 1f lock-in signal was the most definite of the three F_g=2 zero-crossings. By locking at this frequency, the range of frequency shift needed to obtain spectra of the ^{39}K F_g=1 and ^{41}K F_g=2 transitions coincided with the range of maximum efficiency for the first-order diffraction though the 380MHz AOM.

Before using the final method involving a beam for locking and a beam for

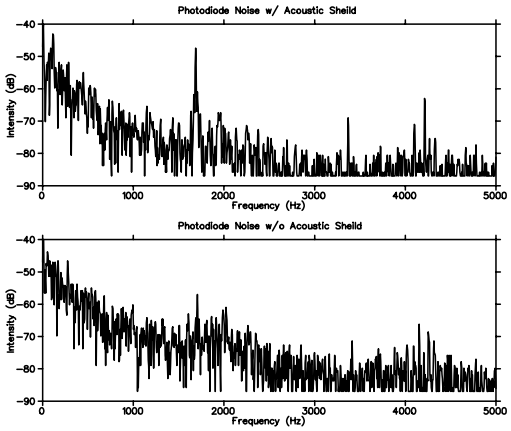

Figure 9: Noise Spectrum Improved by Introduction of Acoustic Shield

sweeping with an AOM, data was taken by sweeping the laser with the scan control unit. The output of a lock-in amplifier that was connected to the photodetector was plotted on a digital oscilloscope. This method suffered from problems related to drifting. The linearity of frequency with the sweep voltage of the laser was not known. Linearity of the recorded sweep voltage with frequency was also affected by the laser's frequency drift, introducing an unknown error to any calibration made from the known ^{39}K line. Laser drift also prevented the suppression of noise through multiple sweeps. One previous result, which was obtained by averaging the calculated isotope shifts from thirty-nine different recorded sweeps, was obtained by a former co-op student working with TRINAT[16]. This result, 454.9±0.2(stat)±1.6(sys)MHz, is believed to have underestimated systematic errors associated with the MOT perturbation of trapped atoms[2]. In agreement with this result was another isotope shift measurement of 454±5MHz that was obtained by Shawn Fostner at TRINAT[9], although the same work also measured a ^{41}K/^{39}K isotope shift of 433±5MHz due to the systematic error of sweeping the laser directly. The initial measurements made by sweeping the laser directly and recording data with a digital scope yielded isotope shifts ranging from 453.58±1.24(stat)MHz to 458.4±3.3(stat)MHz with unknown systematic errors.

The isotope shift was also measured using data collected from photoionization counts in the MOT (the same type of data presented in Figure 13). The pump beam was linearly polarized during this data collection. This method is similar to the final method that was used in that the 405nm laser was frequency locked to the ^{39}K F_g=2 cross-over transition and the laser light used to excite the transitions was shifted by a known amount with a computer-controlled AOM. The isotope shifts calculated from different data collection runs were affected by low count rates, unstable laser locks and frequency bins of width 1.2MHz. Results of 455.35±0.55(stat)MHz and 456.89±0.42(stat)MHz from runs 1216 and 1218, respectively, had unknown systematic errors associated with them, but were encouraging due to their modest agreement with previous results.

The previously discussed method of splitting the laser light, using one beam for frequency-locking and the other for probing the transitions of interest, is believed to have produced the most accurate and precise measurement of the ^{41}K/^{39}K isotope shift. An external signal amplifier and external lock-in amplifier were used to obtain a measurable 1f [11] lock-in signal from the beam swept with the AOM. The systematic error of this method is only affected by the laser width and the degree to which the lock frequency is known. Several runs of data were taken to optimize the lock-in's time constant, sensitivity, and phase, as well as the rate at which the AOM swept the laser frequency. To calibrate the AOM frequency as a function of the input control voltage, several voltage-frequency data points were taken and a polynomial fit was made to the data (see Figure 10). Because the DAC connected to the computer controlling the AOM frequency had a range of only -5 to 5V, an encased battery was connected between the output the DAC and the AOM amplifier to provide a clean DC offset. The decrease in frequency due to the gradual discharge of the battery was noted to be ∼0.2MHz per day. As such, this calibration is only applicable to data obtained on the same day.

After locking the laser, the AOM was swept over the frequency range of interest with a DAC connected to a control PC. An ADC connected to the PC

[11] 1f, in this context, implies that the lock-in signal is effectively the first derivative of the input signal

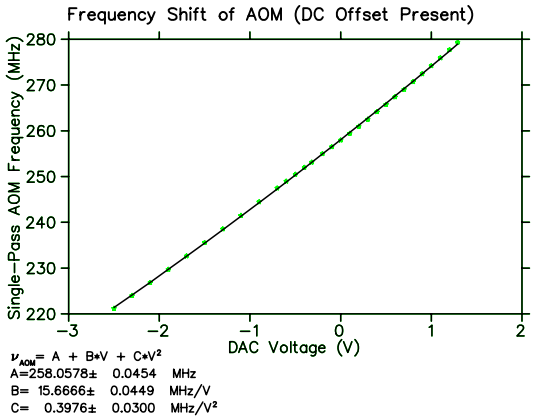

Figure 10: Polynomial Fit to Single-Pass AOM Frequency Shift as a Function of Control Voltage

provided a means of data collection. The PC was set to take 1000 samples per point and to record 1024 data points of the lock-in signal and the AOM control voltage. The time constant of the external lock-in amplifier was set to τ =3ms and the sensitivity to 1mV. For each run, data was taken for several minutes to lower noise and better resolve structure. First, the AOM was set to sweep a range of 221 to 279MHz (single pass frequency shift), showing both ^{39}K F_g=1 and ^{41}K F_g=2 transitions. A run with a lock-in phase shift of 90° was also made. The phase setting was returned and shifted beam was then deliberately misaligned so that it did not travel along the pump beam and, as such, showed only the background structure, absent of the fine structure of interest. This data is thought to show the background, which depends on the varying AOM efficiency. Data was then taken of only the ^{41}K F_g=2 transitions, with the AOM swept between 253 and 279MHz. Further runs were made with the AOM shifting the laser light to higher values to show ^{41}K F_g=1 structure.

The weighted mean of the centroid of four fits to the ^{41}K F_g=2 lock-in peaks was 535.69MHz (see Figures 11 & 12). This value is the amount the double-pass AOM shifted the laser light between the locked ^{39}K F_g=2 cross-over fre-

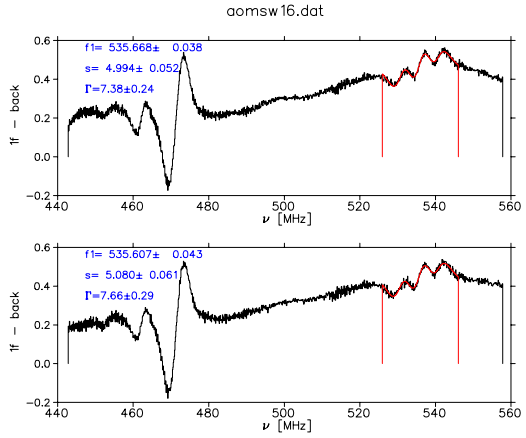

Figure 11: ^{39}K F_g=1 and ^{41}K F_g=2 Lock-in Signal (Data Run 16)

quency and the cross-over of the ^{41}K F_g=2 transitions. Due to the relative offsets of these two levels from each isotope's so-called COG,[12] a subtraction of 78.89MHz (determined using the Hyperfine A constant values from [1] and scaling by the nuclear magnetic moment[2]) is made. This results in an isotope shift of 456.1±0.75MHz.

Source of Error	ϵ (MHz)
Variation When Phase Shifted 90°	0.15
Lock Point Uncertainty	0.35
Subtraction of Background	0.10
Opposite Sweep Directions	0.07
Variation Between Runs	0.08
Total	**0.75**

Table 3: Sources of Errors in Calculation of Isotope Shift

The error of the reported result has five contributing factors. Fits of the

[12]The "Centre of Gravity" is defined as the frequency of the transition, in this case, the $4S_{1/2}$-$5P_{1/2}$ transitions, with the hyperfine interaction artificially set to zero.

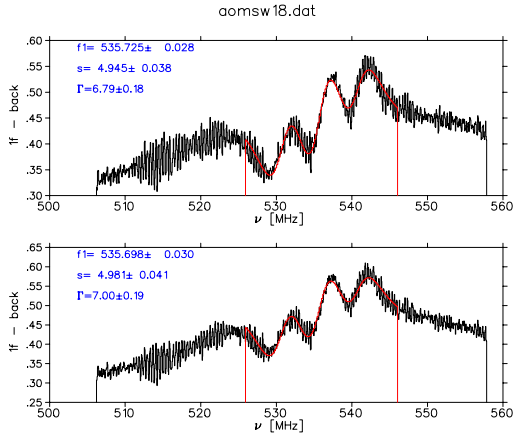

Figure 12: ^{41}K F_g=2 Lock-in Signal (Data Run 18)

derivative of three Lorentzian curves (the expected 1f lock-in distribution for the trio of F_e=1, F_e=2, and cross-over transitions) with a linear background were made to the data that showed ^{39}K F_g=1 curves. As the separation of ^{39}K transitions is known well, this helped to calibrate the lock point. The centroid of the fit to this structure revealed that the lock point was low by 0.7MHz. Half of this value was added to the total error to account for uncertainty in the exact frequency of the laser lock. Because the fit to the data that was taken with the phase shifted 90° differed by ∼0.15MHz from the final isotope shift value, a contribution of 0.15MHz was added to the error estimate. Fits made to the ^{41}K F_g=2 transitions with and without the background subtracted did not show much variance in the centroids. The small difference between fits made with a background subtraction and those made to the raw data lead to a contribution of 0.10MHz to the error of the isotope shift. Similarly, a small contribution to the error came from the differences in the isotope shift calculated from the fits made to each data run and the differences in the calculated isotope shift from the fits made to the first (positive frequency sweep) and second (negative frequency sweep) halves of each sweep. To be conservative in estimating the error, all contributions were added linearly (see Table 3). The final error, ±0.75MHz, is assigned to the determined ^{41}K/^{39}K isotope shift.

Data obtained of the ^{41}K cross-over ($F_g = \frac{1}{2}$) transitions was analyzed in a similar fashion. A much lower s/n ratio was found for the cross-over transitions. This is believed to be due to the poor first-order diffraction efficiency of the AOM at the frequency range required to observe the cross-over peak (∼318-346MHz) and the weaker strength of the transition. The fits made to this data had higher uncertainties on the centroids than those made to the F_g=2 transitions and appeared much worse visually; however, the isotope shifts calculated from the this data were in agreement with our final result. Because of the low s/n ratio and the higher uncertainty, the cross-over data is viewed as encouraging, but not adequate for inclusion in the final analysis.

As introduced in Section 3.3, the isotope shift is comprised of three components, the normal mass shift, specific mass shift, and the field shift. By subtracting the normal mass shift from the total isotope shift, the sum of the field shift and the specific mass shift (known as the residual isotope shift) was determined:

$$RIS = FS + SMS = \Delta\nu_{iso} - NMS =$$
$$456.1\pm0.75\text{MHz} - 508.8\text{MHz} = -52.7\pm0.75\text{MHz}$$

The field shift for the $4S_{1/2}$-$4P_{1/2}$ transitions has been calculated using the electronic factor of the field shift, F=-110±3MHz fm^{-2}, and the SMS constant, k_{SMS} = -15.4±3.8GHz amu, to be -12.91±4.93MHz[14]. As this is dominated by the $4S_{1/2}$ state, it can be scaled using the hyperfine A coefficients:

$$FS_{4s_{\frac{1}{2}}\rightarrow 5p_{\frac{1}{2}}} = FS_{4s_{\frac{1}{2}}\rightarrow 4p_{\frac{1}{2}}}\left(\frac{F_{4s_{\frac{1}{2}}} + \frac{A_{5p_{\frac{1}{2}}}}{A_{4p_{\frac{1}{2}}}}F_{4p_{\frac{1}{2}}}}{F_{4s_{\frac{1}{2}}} + F_{4p_{\frac{1}{2}}}}\right)$$

After scaling, the field shift of the $4S_{1/2}$-$5P_{1/2}$ transitions is estimated to be -13.31 ± 5.08MHz. This implies a specific mass shift of -39.4 ± 5.13MHz. The error of the specific mass shift is dominated by uncertainty in k_{SMS}, which is the expectation value of $\sum_{i>j} \mathbf{p_i} \cdot \mathbf{p_j}$ (where $\mathbf{p}$ is the momentum of a single electron), of the ground state minus that of the excited state[14]. The value used in the cited work is based on muonic X-ray data and is believed to be the most precise result currently available.

A precise measurement of the hyperfine A coefficient for ^{41}K $5P_{1/2}$ is not known to have been previously made. Scaling the $4P_{1/2}$ hyperfine A constant by the magnetic moment approximates the $5P_{1/2}$ hyperfine A coefficient to be 5.06MHz. From the data presented in figures 11 & 12 a measurement of the hyperfine A coefficient for the $5P_{1/2}$ state was made. The weighted average of the data was found to be 4.96±0.17MHz. A check of the validity of this measurement was made by calculating the hyperfine A coefficient for ^{41}K $5P_{1/2}$ from the data. This was found to be 8.983±0.14MHz, in excellent agreement with the previous best measurement of 8.99±0.15MHz [10].

5.3 Ground State Populations in Polarized ^{41}K

As previously explained in Section 4.4, in order to determine the ground state populations of the atoms in the MOT, a 405nm and a 532nm laser were used to linearly excite the atoms from the ground state and to photoionize the excited atoms. To excite the ^{41}K F_g=2 transitions, the laser was locked to the ^{39}K F_g=2 cross-over peak. The 380MHz AOM was set to shift the laser light by thirty-six steps. The DAC output from the control PC was offset with a DC voltage and varied between −0.32V and 1.29V, corresponding to an AOM shift range of ∼253 to ∼280MHz, varying slightly day-to-day due to the slow discharge of the offset battery.

To excite the ^{41}K F_g=1 transitions, the laser had to be locked to one of the F_g crossover transitions. The most stable lock was found to be the crossover of these resonances, F=$\frac{1}{2} \rightarrow \frac{1}{2}$. In order to lock to this group of transitions, the phase setting needed to be adjusted by 180° so that the lock-in amplifier would lock to the negative-slope zero-crossing. The lock-in offset also needed to be adjusted due to the fact that a Doppler background was present, causing the different offset at each group of peaks to be present.

The control PC also controlled both the timing of the 767nm push beam (see Section 4.1) and the polarization of the 770nm optical pumping beam (see Section 4.3). For each step of the DAC controlling the 405nm AOM, the 770nm beam was switched through σ^+, σ^-, and linear polarizations. The data was processed with NOVA, and data files for each 770nm polarization containing in-

formation of the number of counts at different 405nm AOM shifts were written to disk. This data had basic Poisson statistical errors associated with it. To normalize this, data that was thought to be proportional to both the number of atoms in the MOT and the 405nm beam intensity (which varies with AOM shift) was also written to disk.

After the first complimentary data runs of the ^{41}K F_g=1 and F_g=2 transitions were taken, normalization of the data showed the F_g=1 peaks to be more intense than the F_g=2. It was previously expected that the majority of the electrons would be in the F_g=2, m_F=2 state for σ^+ polarization and F_g=2, m_F=-2 for σ^-. To check that the normalization was correct, another method of normalization was attempted. Data from a camera with a 767nm filter aimed towards the atoms in the second MOT was used as a gauge of the number of atoms in the MOT. The 405nm AOM's transmission at different frequencies in its orientation at the time of the runs was also recorded. Normalization to both of these resulted in similar distributions to what had been observed when the data processed in NOVA was used. It was decided that the original method of normalization was resulting in an accurate picture of the atoms' ground-state populations.

The data was read with a script written for PHYSICA[13]. The data had to be rebinned to thirty-six (the amount of steps taken with the 405nm AOM) bins because many counts were recorded in two adjacent bins and fits could not be made with blank values present. In order to fit the linear data, even populations were assumed for each of the Zeeman-split sublevels with the same quantum number F. For σ^+ polarized light, the ground state populations were limited to the F_g=2, m_F=2,1 and F_g=1, m_F=1 states (see Figure 2). Likewise, for σ^- polarized light, the ground state populations were limited to the F_g=2, m_F=-2,-1 and F_g=1, m_F=-1 states. In all fits, the Lorentzian half-width, Γ, as well as the centroid and magnetic field along the quantization axis, were allowed to vary. This totals six variable parameters in the fits to σ polarization and five in those to linear polarization. More information could be obtained if all populations had been allowed to vary; however, PHYSICA's fit routine failed when more than six parameters were used.

[13]PHYSICA is a data analysis and display program developed at TRIUMF.

The fits to the linear data resulted in a ratio of total F=2 population to total F=1 population of 0.83±0.10. It is believed that limiting the ground state populations of the same F to be equal is an oversimplification of the true situation. Graphically, the fitted curves appear to fit the data fairly well, but also reveal to what extent the necessary limitation on the population levels differs from the true picture. The regions in which the curve most disagrees with the data are those in which a slightly higher number of atoms in states with $m_F = \pm 1, \pm 2$ would lead to an improved fit. It is believed that when optically pumping with linearly-polarized 770nm light, the atoms become polarized to some extent, although very little net polarization results. The reported value of 1.25 for $\langle m_i^2 \rangle$ in Figure 13 is believed to be lower than the true value when optically pumping with linearly polarized light.

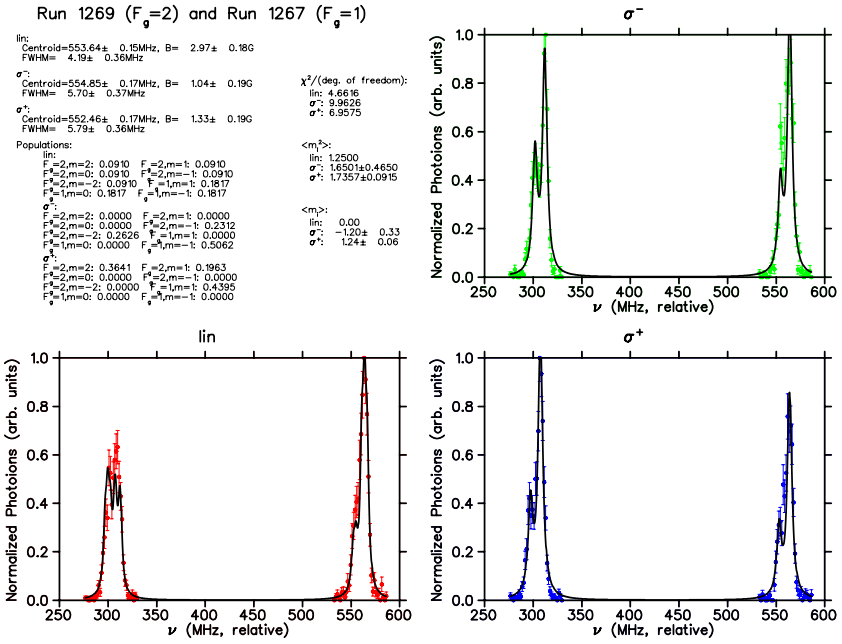

Figure 13: Combined Data From Runs 1267 & 1269

Curves fitted to the σ^- and σ^+ data, limiting the electrons to only three states, agreed with the data surprisingly well. The fits to the F_g=2 data agree very well and support the assumption that the vast majority of F_g=2 electrons are in the m_F=2,1 magnetic substates for σ^+ and m_F=−2,−1 for σ^-. The higher frequency, F_g=1, transitions show similar disagreements between the fitted curves and the data in both σ^- and σ^+. The observed F=1 → 1 peaks are stronger then the fitted curves imply (see Figure 3 for the relative strengths of these peaks for even ground state populations). Because of the relative weights of the transitions (see Appendix D of [15]), it is not possible to further increase the strength of these transition with respect to the F=1 → 2 transitions. The implications of this disagreement are not fully understood. The model assumed that the mixing of Eigenstates with the same F value due to off-axis magnetic field components were negligible. It is likely this is not the case. For a 1Gauss field, the mixing of the $5P_{1/2}$ states would result in a ∼5% effect for F=2 and ∼15% for F=1[2]. Further analysis of this quantum mechanical effect needs to be done to fully understand the effect of off-axis magnetic field components.

Further fits were made to counts of photoions in coincidence with the pulsed 355nm laser from the time the optical pumping light is on (see Figure 14). These fits were in reasonable agreement with the population ratio of F_g=2 to F_g=1 electrons mentioned above, giving a value of 0.67 with an undetermined error. In other areas, these fits, which were made by purposely spoiling the polarizations, were in strong contrast to the previously discussed 405nm photoion fits. The fits to σ^+ and σ^- polarizations resulted in ∼50% of the electrons populating the F=2, m_F=2 state for σ^+ and ∼50% in the F=2, $m_F = -2$ state for σ^- state. This is in stark contrast to the populations determined in from the 405nm photoions. The determined polarizations are ∼55% and − ∼55% for σ^+ and σ^- polarizations, respectively. These are less than those determined from the 405nm photoions, although, as previously stated, those values are artificially high, due to the necessary limitations on the fit. The $\langle m_i^2 \rangle$ values from the photoions coincident with the 355nm pulses, ∼1.65 for both σ polarizations, were in agreement with those made from the 405nm photoion data. Similar fits to this data, varying the magnetic field rather than the quality of the polarization, resulted in high populations of the m_F=0 magnetic substates. As this contrasts with the result obtained from the 405nm photoions, wherein the

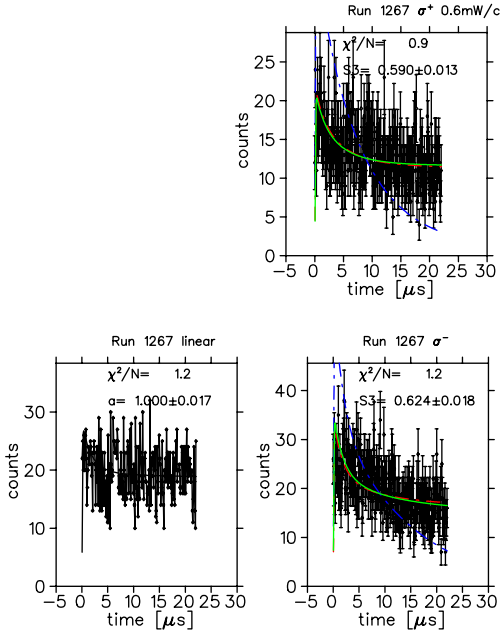

Figure 14: Photoions Coincident with 355nm Pulses

$m_F = \pm 1, \pm 2$ substates were believed to be preferentially populated, the fitted model is thought to require further development.

6 Conclusions

The increase in energy between the $4S_{1/2}$-$5P_{1/2}$ transition of ^{41}K and that of ^{39}K was measured using the methods of saturation spectroscopy and lock-in amplification to be 456.1±0.75MHz. This value contrasts with the estimated value of 476.8MHz, which was calculated using $4S_{1/2}$-$4P_{1/2}$ data from [14]. The error assigned to the measured isotope was determined very conservatively and is less than half the amplitude of the smallest of errors presented in previous TRINAT studies as well as other values determined in this work. A specific mass shift of −39.4±5.1MHz, determined from the measured isotope shift, is limited

in its precision by the muonic X-ray data by [22] used in [14] to calculate the $4S_{1/2}$-$4P_{1/2}$ field shift. The field shift is believed to be dominated by the ground state and, as such, a scaling of only ∼3%, based on the ratio of the hyperfine A coefficients of the $4P_{1/2}$ and $5P_{1/2}$ states, was needed. To improve this value, a more precise measurement of the specific mass shift must be determined. An unexpected extra result of this study was the determination of the hyperfine A coefficient of the $5P_{1/2}$ state of ^{41}K to be 4.96±0.17MHz. This is limited by electronic noise, acoustic noise and laser lock stability.

By optically pumping trapped atoms with the 770nm diode laser, the atoms become polarized through the mechanism described in Section 4.3 and illustrated in Figure 7. This polarization can be determined to an extent by fitting Lorentzian-distributed transition peaks. Polarization does not reveal the true picture of the polarized atoms because of the range of different ground state population schemes that will result in the same value of polarization. As such, the analysis presented here attempts to draw further conclusions about the distribution of the electrons' states in the trapped atoms.

It is believed that during optical pumping with linearly-polarized 770nm light, the electrons have a tendency to be redistributed to the $m_F = \pm 1, \pm 2$ states, increasing $\langle m_i^2 \rangle$ for the trapped atoms to higher values than the 1.25 presented (due to the previously discussed restrictions on the populations in the model). With σ^+ and σ^- polarized light, the fitted model had to be restricted to only three populated states for each polarization. Because of this, the $\langle m_i^2 \rangle$ values presented in Figure 13 should be interpreted as upper limits. It is almost certain that all three polarizations of optical pumping light are populating the F=1 ground state to a higher degree than the F=2 state. One point of concern is the disagreement of the model with the data in the F=1→1 region. It is possible that a better understanding of the magnetic field in the MOT, especially that which is produced by the quadrupole, will resolve this discrepancy. The off-axis components of the magnetic field, which are highly dependent on the position of the trapped atoms, may be mixing the magnetic substates to an unknown degree.

7 Acknowledgments

I would like to thank John Behr for his guidance throughout the entire term. During my four month stay at TRIUMF, I learned a great deal about optics, atomic & nuclear physics, and electronics, much of it as a direct result of John's help. The financial support of NSERC and the NRC for my co-op term with TRINAT should also be acknowledged. I would also like to wish the best of luck to the TRINAT group in its future endeavours.

References

[1] E. Arimondo et al., *Rev. of Mod. Phys.*, **49**, 31 (1977)

[2] J.A. Behr, *Personal Communication* (Spring 2006)

[3] J.A. Behr, *Distributed Notes from UBC PHYS522 Lectures*, unpublished (Jan. 2006)

[4] J.A. Behr et al., *Eur. Phys. J. A direct* (online only), **25**, s1.685 (2005)

[5] J.A. Behr, *Nuc. Instr. & Meth. in Phys. Research B*, **204**, 526 (2003)

[6] S. Chu, *Rev. of Mod. Phys.*, **70**, 685 (1998)

[7] C. Cohen-Tannoudji, *Rev. of Mod. Phys.*, **70**, 707 (1998)

[8] A. Corney, Atomic and Laser Spectroscopy, Clarendon Press, Oxford, UK (1977)

[9] S. Fostner, *Co-op Work Term Report*, TRIUMF/Univ. of Guelph, unpublished, (Mar. 2004)

[10] W.N. Fox & G. W. Series, *Proc. Phys. Soc. Lond.*, **77**, 1141 (1961)

[11] L.J.S. Halloran, J.A. Behr, S. Fostner & E. Paradis, *Can. Jour. Phys.*, (in preparation, April 2006)

[12] L. Hollberg & M. Ohtsu, *Appl. Phys. Lett.*, **53**, 944 (1988)

[13] A-M Mårtensson & S. Salomonson, *J. Phys. B: At. Mol. Phys.*, **15**, 2115 (1982)

[14] A-M Mårtensson-Pendrill et al., *J. Phys. B: At. Mol. Opt. Phys.*, **23**, 1749 (1990)

[15] H.J. Metcalf & P. van der Straten, Laser Cooling and Trapping, Springer-Verlag, New York, NY (1999)

[16] E. Paradis, *Co-op Work Term Report*, TRIUMF/Univ. of Waterloo, unpublished (Dec. 2003)

[17] W.D. Phillips, *Rev. of Mod. Phys.*, **70**, 721 (1998)

[18] E.L. Raab et al., *Phys. Rev. Lett.* **59**, 2631 (1987)

[19] T.B. Swanson et al., *J. Opt. Soc. America*, **15**, 2641 (1998)

[20] M. Weel & A. Kumarakrishnan, *Can. J. Phys.* **80**, 1449 (2002)

[21] Wikipedia, "Acousto-Optic Modulator," `http://en.wikipedia.org/wiki/Acousto-optic_modulator`, (last accessed: Apr. 2006)

[22] H.D. Wohlfahrt et al., *Phys. Rev. C*, **23**, 533 (1981)

[23] J.L. Wiza, *Nucl. Instr. & Meth.* **162**, 587 (1979)

A Laser Lock Monitoring Program in C

The initial runs of data taken this term were subject to a very unreliable frequency lock of the 405nm laser. This would often stay locked for only a few minutes and rarely for more than fifteen minutes. The indicator of when the laser had gone out of lock was a lack of new counts being taken by the data acquisition. Data obtained in this manner had to be processed by cutting out all data obtained after a certain point in the run time, and then combining files. To fix this, a program, `alar405.c`, was written, using excerpts of code created by former TRINAT personnel as a starting point, that monitored the lock-in voltage.

This program monitors the PID voltages of the 405nm and 770nm (which also goes out of lock, though far less frequently) lasers. It prompts the user for three values. The parameter `iave` is the number of samples the program takes when measuring the lock-in voltage. A value of 1000 causes the program to run at about 2Hz (i.e., it measures the voltages twice each second) and seems to be a good trade-off between speed and stability of the program. The other two parameters set upper limits on how much the lock-in voltages can vary between each voltage measurement. If laser comes out of lock, the Toptica LIA110/100 will sweep the voltage until it finds another suitable lock point. The values 8mV and 15mV for the 405nm and 770nm, respectively, seem to be able to detect when the laser comes out of lock and re-locks on an adjacent peak, but not to falsely trigger the program to report an out-of-lock laser. When the program

detects a laser is out of lock, it sends a -2V signal on ADC0 of the control computer, which will pause sweeping of the 405nm AOM frequency and the switching of the 770nm polarization. The data acquisition computer also reads this -2V signal into its C212 logic. an *if* statement within the `green*.ncm` analysis files prevents the incrementing of any of the scalars until the control computer is told to continue (with 2 hits of `enter`).

B Hints for Finding Resonances, Tweaking PZT & Current

To find resonances of ^{39}K with the 405nm, adjustments to two controls, the laser diode current and the PZT offset, need to be made. When the laser is turned on, it should return to $\sim$27.7°C and $\sim$55mA, both displayed on the Toptica control unit. There are two lasing modes that give good single-mode power to the frequency of interest. The location of these varies day-to-day; however, one can always be found in the region where the current LCD displays 54mA, the other at 55mA. The 55mA region seems to give brighter fluorescence, which means more power in the main mode is being delivered to the cell, although both current regions can be made to lase single-mode.

To find the resonances, it is useful to set the scan control to sweep, turning the amplitude control to about half its full value. If the PZT offset is at a reasonable value (this varies with temperature), the current control should then be varied until a flash appears on the screen. After setting the sweep amplitude to zero, an adjustment to the PZT offset should be made. Once a flash occurs and there is strong (almost saturating the camera) fluorescence, the current control should be optimized. The current region in which the laser will lase single-mode (this can be viewed on an oscilloscope from the Wavemeter Jr. output) is $\sim$15 units of the current control potentiometer (with a current range setting of 4). The laser hops out of mode suddenly on the lower current end of this region. To return it to the correct mode, a larger positive adjustment needs to be made due to the hysteresis-like behaviour of the laser. On the high side of the current region, the laser gradually exhibits multi-mode behaviour. This can be avoided by setting the current control approximately half-way between higher the point where the laser becomes multi-mode and the lower point where

the laser hops modes. At the time of writing, optimum settings are: current range=4, current=754, PZT offset=396-410.

C Relevant Files and Scalars For Ground State Population Analysis

File	Location	Description
`fitall7.pcm`	`midtis01:/home/trinat/nova/lh/21apr06`	PHYSICA fitting routine that takes F_g=1 and F_g=2 data files as inputs
`swrite.ncm`	`midtis01:/home/trinat/nova/lh/`	NOVA script to write out relevant scalars (see Table 5)
`*.*`	`melconpc:/home/landonh/coopreport`	all files that make up this report
`*.*`	`ibm00:/home/landonh/aomsw`	all ^{41}K spectroscopy data
`green14.ncm`	`midtis01:/home/trinat/nova/`	NOVA script file used in the final analysis

Table 4: Relevant Files for Ground State Population Analysis

Scalar Name	Description
`sdacphotom`	MOT on photoions
`sdacphotoo`	MOT off photoions
`sdacphotomen`	normalization for `sdacphotom` or `sdacphotoo`
`spcdacphotom`	σ^- photoions
`spcdacphotop`	σ^+ photoions
`spcdacphotol`	linear photoions
`sdacphotomnm`	normalization for `spcdacphotom`
`sdacphotomnp`	normalization for `spcdacphotop`
`sdacphotomnl`	normalization for `spcdacphotol`

Table 5: Notable Scalars from NOVA Analysis Files

All scalars listed in Table 5 are from `green14.ncm`.